Intermolecular MH···HR Bonding in Monohydride Mo and W Complexes

Galina Orlova[†] and Steve Scheiner*

Department of Chemistry, Southern Illinois University, Carbondale, Illinois 62901

Received: August 20, 1997; In Final Form: October 17, 1997[⊗]

Intermolecular interactions between HR (R = F, OH, H_2O^+) and the hydride and NO ligands of Mo(H)$(CO)_2(L)_2(L')$ (where cis-ligand L = PH_3, NH_3; trans-ligand L′ = NO, Cl, H) and the $W(H)(CO)_2(NO)(PH_3)_2$ complex have been studied using HF/3-21G and DFT (B3LYP, BLYP, B3PW91) methods. The structure of the complexes depends upon the nature of the trans-ligand and the proton donor ability of HR. H···H bonding exists in the case of poor and moderate proton donors HR and the strong π-acceptor trans-ligand. A strong σ-donor cis-ligand strengthens the H···H bonding. The change from poor proton donor to strongly acidic HR leads to a η^2-H_2 structure. The dihydride structure is formed with replacement of a π-acceptor trans-ligand by a σ-donor as a result of greater nucleophilicity of the metal atom. Energy decomposition analysis shows that the H···H bond consists of a large electrostatic component, with a small but significant contribution from both charge transfer and polarization, distinct from the pattern of the conventional H-bond wherein polarization makes a more minor contribution. Whereas HF/3-21G predicts a preference for a H···O interaction, the DFT approaches favor H···H. B3PW91 results are in the best agreement with available experimental data.

Introduction

Recent years have witnessed the introduction of a new idea into the lexicon of molecular interactions. It has been suggested that a hydrogen atom, when bound directly to a transition metal, can acquire sufficient electron density that it can act as a proton-acceptor atom in a sort of hydrogen bond. This novel M−H···HR intermolecular bonding has been examined theoretically by Liu and Hoffmann, who categorized it as very weak, consisting mainly of an electrostatic interaction.[1] The Crabtree[2] and Epstein and Berke[3,4] groups have used methods of spectroscopy (IR, NMR, neutron diffraction) to study candidate complexes, for M = Re, W and HR = indole and acidic alcohols, in transition-metal hydrides **1**−**3**. This H···H bonding is unexpectedly strong and is preferred over possible NO···HR and CO···HR interactions for **2** and **3**, although the latter may be present as well. According to IR and NMR data,[4] the H···H interaction in **2** accounts for about 4−7 kcal/mol; the pertinent distance is in the 1.7−1.9 Å range. Consistent with patterns in normal H-bonds, the strongest bond was associated with the most basic ligand (L) and the most acidic HR. The H···H interaction in complexes **1**−**3** appears to represent new evidence of the nucleophilic character of the hydride hydrogen. It was shown via NMR by Richmond et al. in 1982[5] that the reactivity of metal carbonyl hydrides with strong Lewis acids is dominated by the basic character of the hydride ligand. The hydride ligand appears to be the more basic site compared to the carbonyl oxygen, even in relatively acidic hydrides such as $HMn(CO)_5$.

The H···H-containing transition-metal complexes may play an important role in the chemistry of hydrides as intermediates or transition states on the pathway of proton transfer in reactions of hydrides with proton donors. An interesting application might be the possibility of using such complexes as recognition probes,[2] taking advantage of the extraordinary sensitivity of the H···H bond to the nature of ligands.

Although some of these experimental trends have been confirmed in large measure by DFT calculations,[2,4] the results of both experimental and theoretical investigations[2,4] remain controversial. For instance, according to spectroscopic data[3,4] of complex **2** and DFT calculations[4] of a model of compound **3**, the H···H bond prefers a linear geometry. In contrast, according to neutron diffraction data[2] of complex **1** and DFT calculations[2] of a model of this complex, a three-center NH···H_2-Re bond is present, quite distinct from linear. The fundamental nature of the H···H interactions and the reasons for preference of H···H over other possible interactions in transition-metal complexes are not yet resolved. We attempt in this communication to elucidate the structure and particular features of this new type of intermolecular H···H bonding, particularly in contrast to the conventional sort of H-bonds. To study the influence of the nature of the transition metal (M), cis- and trans-ligands (L, L′), and proton donors (HR) on the H···H bonding model, structures **4** and **5** were studied using computational methods.

Methods of Calculation

Accurate computations of complexes containing large transition-metal atoms have presented a computational problem for some time. Modified coupled pair functional (MCPF) methods and coupled cluster [(CCSD(T)] methods[6] would likely be reliable, but the cost of these methods is prohibitive and the size of the systems that can be calculated is limited. On the other hand, transition-metal complexes can be computed to good accuracy using density functional theory (DFT) methods.[7] Indeed, DFT computational results for transition-metal carbonyl hydrides[8] and molecular hydrogen complexes of osmium (II)[9,10] are generally in good agreement with the available experimental data and second-order Møller−Plesset perturbation (MP2) calculations.

[†] Permanent address: Institute of Physical & Organic Chemistry, Rostov University, Rostov on Don, Russia 344090.

[⊗] Abstract published in *Advance ACS Abstracts,* December 1, 1997.

S1089-5639(97)02710-2 CCC: $15.00
Published on Web 01/01/1998

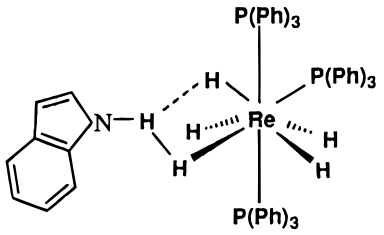

1

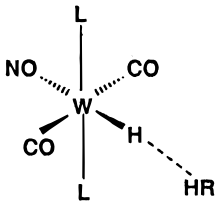

HR=PhOH, $(CF_3)_2CHOH$, $(CF_3)_3CHOH$

L=PMe_3, PEt_3, $P(O^iPr)_3$, PPh_3

2

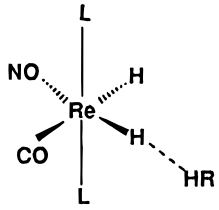

HR=perfluoro-t-butanol

L=PMe_3, PEt_3, $PiPr_3$

3

In the present study we report a frozen-core calculation based on the DFT method as implemented in the GAUSSIAN-94 program.[11] Becke's 1988 (B)[12] and Becke's three-parameter functional (B3)[13] are used to model the exchange. Correlation was included via the functionals of Lee, Yang, and Parr (LYP)[14] and Perdew and Wang (PW91),[15] as a modification of the Perdew−1986 (P86)[16] nonlocal correction (B3LYP, BLYP, and B3PW91). It has been shown[17,18] that nonlocal corrections can improve calculated metal−ligand bond distances considerably in certain cases, but there are not enough data in favor of any one nonlocal correction method. According to an overall perspective,[8] BLYP results for transition-metal hydrides are qualitatively similar to those from BP86. BP86 calculations of transition-metal carbonyls, carbonyl hydrides, and sandwich complexes of Fan and Ziegler[19] are in good agreement with experimental data. On the other hand, BLYP and B3LYP methods underestimate H−H distances by ≈0.3 Å in molecular hydride complexes of Os(II) with strong π-acceptor ligands, in comparison with MP2 values.[9] The identification of the best available nonlocal correction scheme for complexes of transition-metal hydrides containing an intermolecular hydrogen bond is one of the aims of this work.

The standard LanL2DZ double-ζ basis set[20] of the GAUSSIAN 94 package was used. According to computational results for transition-metal carbonyl hydrides and carbonyls,[8] DFT geometries are not very sensitive to the enlargement of the double-ζ basis set to the triple-ζ quality. The HF/3-21G method[21] is used for comparison purposes also. Energies of

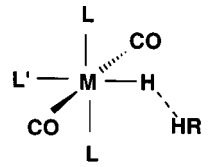

M=Mo, L=PH_3, NH_3, L'=NO, R=F

M=Mo, L=PH_3, L'=Cl, R=F

M=Mo, L=PH_3, L'=H, R=F

M=Mo, L=PH_3, L'=NO, R=OH, H_2O^+

M=W, L=PH_3, R=F

4

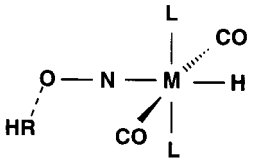

M=Mo, L=PH_3, NH_3, R=F

M=W, L=PH_3, R=F

M=Mo, L=PH_3, R=OH

5

all types of H-bonds were calculated as the difference between the total energy of the complex and the sum of total energies of HR and corresponding hydride. Basis set superposition error was not corrected at this level.

Results and Discussion

1. General Analysis of the H···H Interaction. $Mo(CO)_2(NO)(PH_3)_2H\cdots HF$. As a first step, HF was allowed to interact with $Mo(CO)_2(NO)(PH_3)_2H$. The PH_3 ligands can be considered as σ-donors and the CO and NO groups as π-acceptors. The geometries optimized for these two molecules are reported in Figure 1 at different levels of theory, as indicated in the figure caption. Two principal configurations that might be anticipated for the complex are summarized in Figure 1 as **8a** and **8b**. In both structures, the hydrogen atoms of the two subunits approach one another to form a H···H interaction. In **8a**, the H−F molecule lies in the same plane as the Mo, H, and two P atoms, imparting C_s symmetry to the complex. At all levels of theory, **8a** corresponds to a transition state, with a single negative eigenvalue in its Hessian matrix. Upon relaxation along the transition vector direction,[22] one reaches structure **8b**, only 0.5 (DFT)−2.9 kcal/mol (HF/3-21G) lower in energy. This configuration belongs to the C_1 point group,[23] and the HF molecule lies out of the plane formed by the H, Mo, and P atoms by some 40°. At the HF/3-21G level, **8b** represents a shallow minimum, with lowest frequency 60 cm^{-1}.

The computed interaction energies of **8a** and **8b** are listed in Table 1 from which it may be noted that the DFT values for the latter are in the 11−13 kcal/mol range. These values are probably an exaggeration, at least when compared directly to the experimental estimate of 7 kcal/mol.[3] The HF/3-21G interaction energy is about 5 kcal/mol higher than DFT, likely reflecting the poor quality of this basis set and the HF approximation in general. With respect to geometrical aspects, DFT exhibits the usual overestimation of many of the bond lengths. (For example, the experimental H−F bond length is 0.917 Å.[24]) Although the HF/3-21G method yields somewhat longer H···H distances than the DFT variants, the latter are

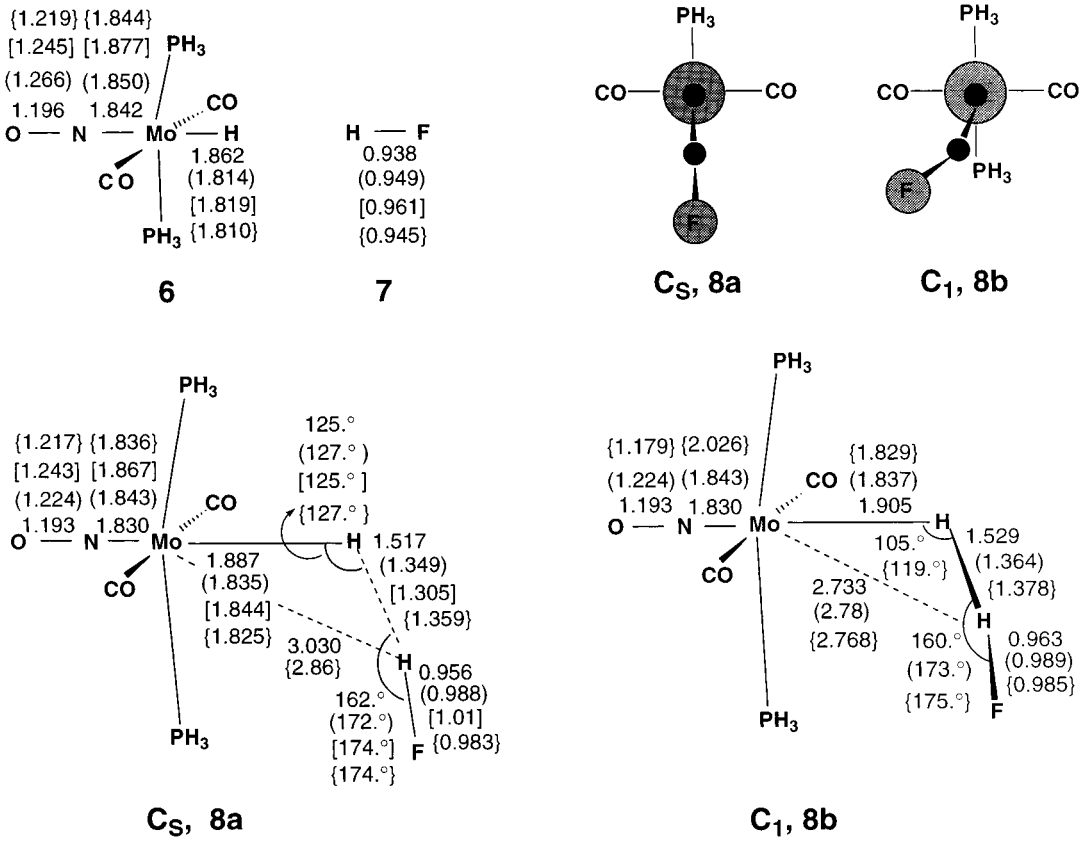

Figure 1. Geometries (in Å and deg) of **6**−**8** computed by 3-21G, B3LYP (values in parentheses), BLYP (square brackets), and B3PW91 (curly brackets) methods.

TABLE 1: Energies of H···H Bonds ΔE_{H-H} (kcal/mol) for 8a and 8b

	ΔE_{H-H}			
structure	3-21G	BLYP	B3LYP	B3PW91
8a	14.7	12.4	12.0	10.5
8b	17.6	12.9	12.4	11.1

remarkably consistent. B3PW91 provides the best results compared to the other DFT methods. As a result of these comparisons, many of the calculations reported below make use of the B3PW91 method.

The most important structural trends are reproduced by both ab initio and DFT methods. For example, both the Mo−H and H−F bonds in complex **8b** are stretched, compared to the isolated subunits **6** and **7**. The amount of this stretch is variable but may be as large as 0.040 Å. The M−H···H bond in complex **8b** is bent, with an angle of less than 120°. When the HF subunit leaves the plane of the Mo and P atoms (**8a**→**8b**), the Mo···HF distance is shortened, but more importantly in terms of any incipient H-bond, the H···H distance is elongated.

Figure 2 depicts the principal characteristics of some of the normal vibrational modes of the subunits and complex. The Mo−H stretching frequency is lowered by 189 cm^{-1} as a result of forming the complex with HF; a red shift of 530 cm^{-1} occurs in HF. The frequencies of modes 29−31, involving the putative H···H bond, lie in the range between 775 and 969 cm^{-1}.

Another window into the nature of this interaction can be opened by examination of charge redistributions that occur as a result of complexation. The overlap populations of the relevant bonds are reported in Figure 3, along with atomic charges in parentheses. Of course, Mulliken charges are sensitive to the choice of basis set and can sometimes give unexpected results,[25,26] since the arbitrary division of overlap

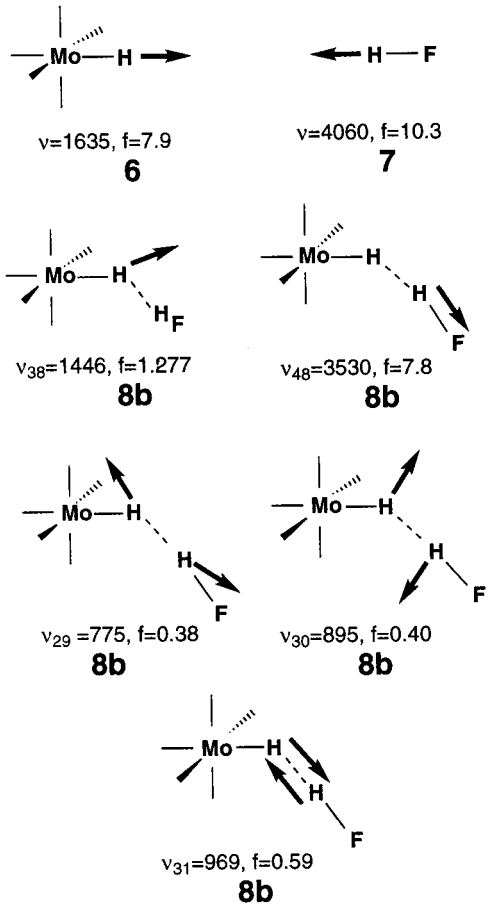

Figure 2. 3-21G harmonic vibrational frequencies (ν, cm^{-1}) and force constants (f, mdyn/Å) for **6**, **7**, and **8b**.

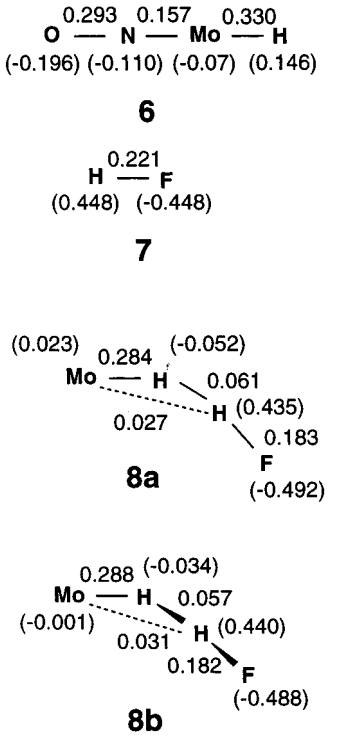

Figure 3. B3PW91 Mulliken overlap populations and charges (values in parentheses) for interacting fragments **6**−**8**.

between atomic centers may be inappropriate, especially for transition-metal complexes. For example, the Mulliken treatment suggests a positive charge on the "hydride" atom of the complex **6**. On the other hand, a Mulliken-type analysis may be quite adequate for studying relative trends, as opposed to absolute charges.[27] Figure 3 indicates that the Mo−H and H−F bonds of **6** and **7**, respectively, are both weakened upon formation of the complex. The overlap of the H···H bond in **8b** is 0.06, about twice that of the M···HF interaction.

One may consider the binding force in the **8b** complex as a competition between three rival forces. First of all, there is an electrophile−nucleophile interaction between the hydrogen atom of HF and the hydride of the metal, by analogy with the three-center bonding MO of a conventional hydrogen bond. The H···H interaction would be expected to increase when the nucleophilic ability of the hydride hydrogen rises, which in turn may be due to a strengthening of the cis σ-donor, here PH_3.

Another sort of force is that between the hydrogen atom of HF and the metal atom. Recall that NO and CO are strong π-acceptors, i.e., electrons can shift into the π^* MOs of these two ligands. This removal of electrons from the metal center will tend to make this atom a poorer electron donor to the HF, weakening the M···HR interaction, which should in turn strengthen the putative H···H bond. These changes ought to be accompanied by a stretch of the M···HR distance and a contraction in H···H. Conversely, weakening of the π-acceptor ability of the trans ligand will raise the π density on M and strengthen the M···HR bond.

A third factor concerns the acidity of HR. One may suppose that, in the case of a strong acid, a structure close to η_2-H_2 molecular complex will be formed when the H···H interaction dominates. The alternate extreme might be a structure closer to a dihydride complex which contains a M···HR interaction. If valid, this scheme opens the possibility that the equilibrium geometry might shift between the two forms by selection of appropriate ligands, transition-metal atoms, and proton donors.

2. Influence of a Strong Cis-σ-Donor. $Mo(CO)_2(NO)(NH_3)_2H\cdots HF$. To test some of our suppositions about the interaction of a transition-metal hydride with HR, the PH_3 ligands of **8** were replaced by the more basic NH_3, forming complex **10a**, illustrated in Figure 4. According to our suppositions, this substitution should lead to strengthening of

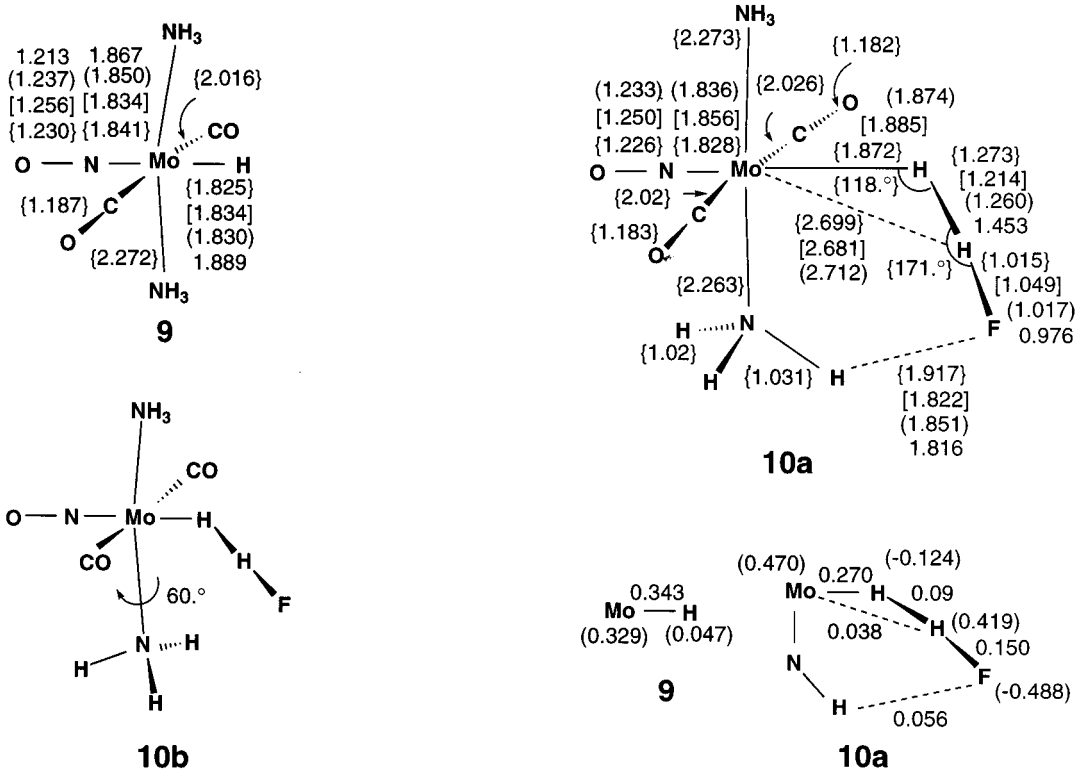

Figure 4. Geometries (in Å and deg), computed by 3-21G, B3LYP (values in parentheses), BLYP (square brackets), and B3PW91 (curly brackets), B3PW91 Mulliken charges (parentheses), and overlap populations in **9** and **10a**.

TABLE 2: Bonding Energies Δ*E* (kcal/mol) for 10a and 10b

	Δ*E*			
structure	3-21G	B3LYP	BLYP	B3PW91
10a	22.5	18.7	20.0	17.1
10b	16.9	16.3	16.9	15.4

the H···H interaction. The structure of **10a**, calculated by HF and DFT, is similar to that of **8b** but has an additional weak interaction between the F atom and one of the hydrogens of NH_3. The distance between these two atoms lies in the 1.8−1.9 Å range, indicative of a weak H-bond. Such complementary interactions between the proton donor and ligands may play an important role in the stabilization of certain complexes. This auxiliary interaction can be intentionally eliminated by rotating the NH_3 group by 60°, yielding structure **10b**. As reported in Table 2, this rotation destabilizes the complex by 1.7 kcal/mol at the B3PW91 level, leaving an interaction energy in the **10b** complex of 15.4 kcal/mol. This quantity is 3.3 kcal/mol higher than in **8b**, indicating a stronger H···H interaction, even with the F···HN interaction deleted. In contrast to all three DFT variants that predict the NH_3 substitution will strengthen the bond, the HF/3-21G calculations are less clear on this point, with an interaction energy difference between **10b** and **8b** of less than 1 kcal/mol.

Further adding to this conclusion of a stronger interaction, the H···H distances are shorter in **10a** compared to **8b**. An aide in this analysis arises from the stretch that occurs in the M−H distances of **9** and **7** upon formation of the pertinent complex. This bond is stretched by 0.044−0.051 Å in the former case, as compared to 0.015−0.025 Å in the latter, verifying the stronger H-bond with the NH_3 ligands. This conclusion of a stronger H···H interaction that accompanies greater σ-donor ability of cis-ligands is in accord with experiment.[3] The overlap population of the H···H bond is also increased as a result of substitution of PH_3 ligands by the more basic NH_3 groups. Interestingly, the overlap population of the M···HF pair is almost equal in **8b** and **10a**.

3. Influence of the Nature of Metal Atom. $W(CO)_2(NO)(PH_3)_2H\cdots HF$. Since there is not much difference between transition metals of rows V and VI, substitution of Mo by W is not expected to lead to major changes. The interaction energy of the tungsten complex **11** (Figure 5) is 11.4 kcal/mol at the B3PW91 level. This computed value is within 0.3 kcal/mol of the same quantity in the molybdenum complex **8b**. The B3PW91 geometry, Mulliken charges, and overlap populations of the C_1 structure **11** are similar to **8b** as well. In an interesting observation, the experimental M−CO bond distance in hexacarbonyls is longer for molybdenum than tungsten.[28] This trend is reproduced by the B3PW91 scheme here. The M−C distances are 2.018 and 2.029 Å for W (**11**) and Mo (**8b**) complexes, respectively. A similar DFT result for Mo−CO and W−CO bonds was reported by Ziegler et al.[29] The lengthening of the H−F and W−H bonds upon formation of complex **11** is close to the corresponding values in **8b**. The H···H distance in the tungsten complex **11** is longer than in the molybdenum complex **8b** by 0.016 Å.

4. Influence of the Acceptor Strength of Trans-Ligand. $Mo(CO)_2(H)(PH_3)H\cdots HF$. As was shown by Jean et al.,[30] the nucleophilicity of the transition-metal atom in octahedral complexes such as **8** is increased considerably when a π-acceptor ligand in trans-position (NO in the case of **8**) is replaced. Indeed, the substitution of a strong π-ligand like NO in **8** by the pure σ-ligand H dramatically changes the geometry of the complex computed by B3PW91. Rather than a structure

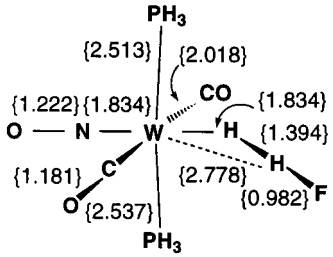

11

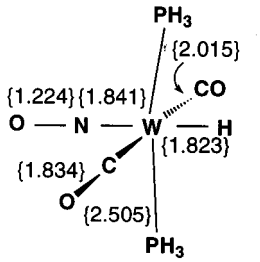

12

Figure 5. B3PW91 geometries (in Å and deg), Mulliken charges (values in parentheses), and overlap populations in **9** and **10a**.

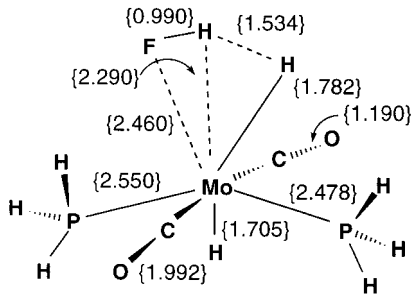

13

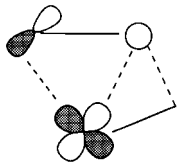

MO 24, **13**

Figure 6. B3PW91 geometries (in Å and deg) and bonding MO, corresponding to agostic interaction of HF and Mo in **13**.

containing a H···H bond, the geometry illustrated by **13** in Figure 6 is obtained, considerably lower in energy.[31] **13** is unique, first, in that the H···H distance is longer. The HF fragment is reoriented so that the F atom is almost as close to the metal atom as is the hydrogen. Indeed, the interaction between the metal and HF can be categorized as an agostic bond, containing an interaction between a π AO of Mo and a bonding MO of the HF bond (see Figure 7). It should also be noted that the replacement of NO by H changes the character of the complex from 18e to 16e. The geometry of the resulting complex **13** is similar to the four-center transition state for the activation of C−H bonds by highly active 16e transition-metal complexes.[31b]

5. Acidity of HR Fragment. $[Mo(CO)_2(NO)(PH_3)_2H\cdots H_3O]^+$. To study the influence of HR acidity, the model structure **14,** formed by interaction of hydride **6** with strongly acidic H_3O^+ was studied at the B3PW91 level. As illustrated in Figure 7, hydronium attacks the hydrogen of **6**, forming a

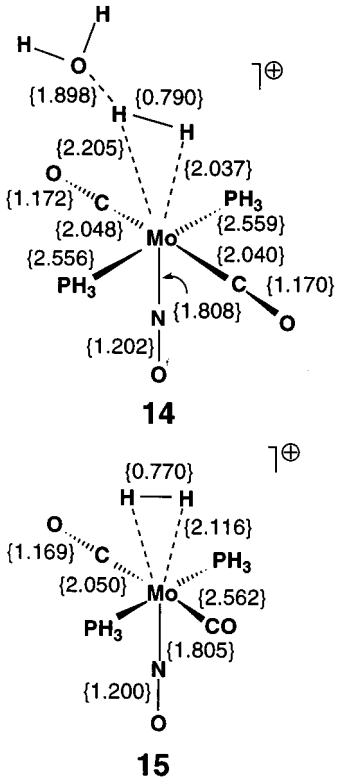

Figure 7. B3PW91 geometries (in Å and deg) of **14** and **15**.

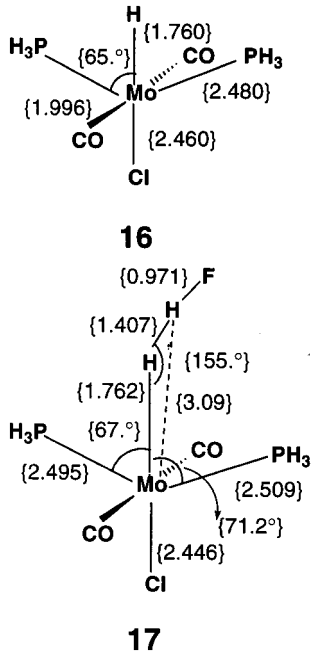

Figure 8. B3PW91 geometries (in Å and deg), Mulliken charges (values in parentheses), and overlap populations in **16** and **17**.

structure that appears to be of η^2-H_2 type. That is, it can be described as a complex involving a H_2 molecule as a ligand, to which is weakly attached a water molecule. The H−H distance in **14** is slightly elongated compared to free H_2 (0.790 vs 0.744 Å). The binding energy of the H_2O molecule in the aqua-η^2-H_2 complex **14** is 19 kcal/mol. The H_2 molecule is weakly bent in complex **14** as compared to the unhydrated **15**. The binding energy of the H_2 molecule in **15** is 9.6 kcal/mol. This result as well as the calculated H−H distance in **15** is close to the experimental and ab initio results of Kubas et al.[32] for η^2-H_2 complexes of Mo. An intermediate corresponding to a H···H sort of complex was not found.

6. Steric Factor. $Mo(CO)_2(Cl)(PH_3)_2H\cdots HF$. As was mentioned above, the H···HR fragments are very "loose": changes of the H···H distance and M−H···H angle do not destabilize the system by much. One might expect, therefore, that bulky ligands can easily alter the structure of the complex without too much energetic cost. The B3PW91 results of a replacement of the NO ligand in **8** by the larger Cl may be seen by **17** in Figure 8. The PH_3 ligands are distorted up and away from Cl, forcing them closer to the hydrogen. This distortion makes it more difficult for the HF to optimally approach the hydrogen. The M−H···H angle in **17** is 36° larger than in **8b.** The calculated energy of the H···H bond in **17** is 6.0 kcal/mol, 5.1 kcal/mol smaller than in **8b.** The H···H distance is also a little longer in **17** compared to **8b**. Part of this weakening may be attributed to the high electronegativity of Cl, which withdraws density from the Mo−H, making this hydrogen a poorer electron donor.

7. Comparative Analysis of the M−H···H and NO···H Interactions. In principle, systems $Mo(H)(PH_3)_2(CO)_2(NO)$ (**6**), $Mo(H)(NH_3)_2(CO)_2(NO)$ (**9**), and $W(H)(PH_3)_2(CO)_2(NO)$ (**12**) are not limited to forming interactions with HF of the H···H type. There are other possible sites for coordination in addition to hydrogen, specifically the oxygen atoms of CO and NO groups, which could form a conventional hydrogen bond with HF. To compare the H···HR interaction with O···HR bonding, structures **18, 19a, 19b,** and **20** in Figure 9 were optimized by HF/3-21G and DFT methods. In addition to the aforementioned FH···O interaction, **19a** is stabilized by an additional F···HNH_3 bond. So as to analyze "pure" H···O bonding of the first sort, model complex **19b** was generated by 60° rotation of the NH_3 group, by analogy with **10b.** HF/3-21G calculations indicate that the $Mo(H)(PH_3)_2(NO)(CO)CO\cdots HF$ complex, where HF interacts with CO, is 9.3 kcal/mol less stable than **18,** where NO···HF bonding exists. Therefore, the NO ligand was chosen for closer scrutiny as a possible site for O···HR interaction.

Equilibrium geometries **18**−**20** involving NO···H bonding have C_s symmetry at all levels of calculation. The structures of these O···H complexes are largely determined by the direction of the lone pair of oxygen.[33] The H-bond energies reported as ΔE in Table 3 demonstrate that the NH_3 ligands make for a stronger interaction than do PH_3, by roughly 3−6 kcal/mol. The quantities labeled $\Delta\Delta E$ in Table 3 refer to the difference in binding energy between these O···H complexes, as compared to the H···H complexes described above. The positive values for the HF/3-21G basis set illustrate that the former is preferred at this level. This behavior contrasts with the three varieties of DFT results which predict the opposite, that H···H binding is favored. In considering how the results might differ at another level of theory, it should be noted that the DFT binding energies of L^z (where $L^z = H_2O$, NH_3, H^-, Cl^-, CN^-, ...) with the metal atom in $[Os(NH_3)_4L^z(\eta^2\text{-}H_2)]^{(z+2)+}$ complexes are in good agreement with MP2 but that the weaker Os···H_2 interaction is underestimated.[8] If the same trend were valid here also, one might expect that the relative stability of the H···H interaction might increase at higher levels of theory.

A comparative analysis of equilibrium geometries underscores certain interesting similarities and distinctions between O···H and H···H complexes. The O···H bond length shortens and the binding energy increases with replacement of PH_3 by NH_3, as was reported in the H···H analogues. The more basic cis-ligand NH_3 increases the nucleophilicity of both the H-ligand and the oxygen atom of NO ligand. The H···O bond shortens and the bonding energy increases also on changing from Mo to W. The nucleophilicity of the strong π-acceptor NO-ligand

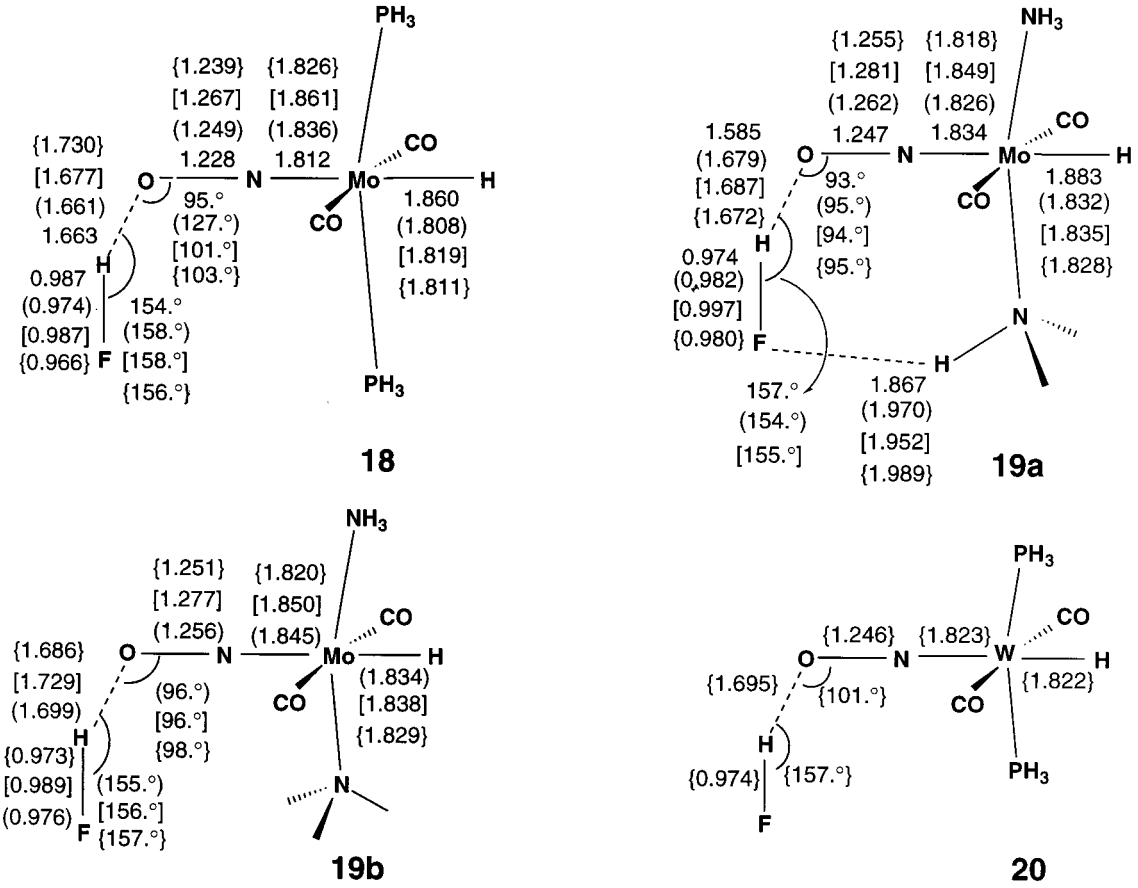

Figure 9. Geometries (in Å and deg) of **18**−**20** computed by 3-21G, B3LYP (values in parentheses), BLYP (square brackets), and B3PW91 (curly brackets) methods.

TABLE 3: Energies of O−H Bonds (ΔE kcal/mol) and Differences of Energies of O−H and H···H Bonds in Corresponding Isomers ($\Delta\Delta E = \Delta E_{O-H} - \Delta E_{H\cdots H}$, kcal/mol) Calculated by 3-21G, B3LYP, BLYP, and B3PW91 for Complexes 18−20

	3-21G		B3LYP		BLYP		B3PW91	
structure	ΔE	$\Delta\Delta E$	ΔE	$\Delta\Delta E$	ΔE	$\Delta\Delta E$	ΔE	$\Delta\Delta E$
18	19.1	1.5	12.0	0.0	11.4	−1.0	9.2	−1.9
19a	27.2	4.7	17.3	−0.8	16.9	−3.1	15.2	−1.9
19b			15.1	−1.1	14.5	−2.4	13.0	−2.4
20							11.2	−0.2

increases more significantly than does the H-ligand with a more basic transition metal. At all levels of calculation, the H−F bond elongates with formation of a H-bond. This stretch is greater for H···H than for O···H with all three DFT variants, consistent with the stronger H···H interaction (3-21G lengths are less consistent).

The Mulliken charges and overlap populations in Figure 10 highlight important differences between O···H and H···H interactions. In either case, the overlap population of the H···H/H···O bond is very small, less than 0.1. In the case of O···H, the negative charge on the oxygen atom and the positive charge on HF *increase* as a result of the interaction. In the case of H···H interaction, the electron density on the hydride hydrogen atom increases, just as the proton acceptor O in the analogous case. However, the positive charge on HF behaves in the opposite fashion, undergoing a decrease. This lowered positive charge can be thought of in the same light as a buildup of electron density, concomitant to formation of the H···H bond.

As indicated above, there appears to be a direct interaction between the HF atom and the central metal. It was thought that perhaps this secondary interaction might bias the comparison between the H···H and O···H bonding in one way or another. In an effort to ameliorate this effect, the HF molecule was replaced by the weaker proton donor H_2O, leading to complexes **21** and **22** illustrated in Figure 11. According to B3PW91, the H···H and H···O distances in **21** and **22** are elongated by 0.3 and 0.2 Å, respectively, compared to the corresponding complexes with HF. The M···H_{H_2O} distance in **21** is longer than 3 Å, certainly minimizing any direct interaction between these two atoms. Complexes **21** and **22** both belong to the C_s point group. The computed H···H distances in **21** and **22** are in good agreement with experimental results[3] and Amsterdam Density Functional package[34] computations of dihydride complex HOH ···HRe(H)(CO)(NO)$(PH_3)_2$.[4] The H···H and O···H binding energies are essentially equal (13.1 and 13.0 kcal/mol, respectively). The reported[4] preference of H···H bonding over O···H is larger (about 3 kcal/mol). The lengthening of the internal O−H bond in H_2O is greater in the case of the H···H complex than O···H, just as noted in the case of HF. Mulliken charges of **21** and **22** differ in an important way from the HF complexes **8b** and **18**. The positive charge on the H_{H_2O} atom *increases* upon formation of the H···H bond, although this increase is less than in the case of HOH···ON. We hence conclude that a principal feature of the H···H interaction is the significant lengthening of the H−R bond.

To provide another perspective on the nature of H···H and H···O bonding, we performed the Kitaura−Morokuma energy decomposition (ED) analysis[35] on simple model complexes HNO···HF (**23**), LiH···HF (**24**), HNO···H_2O (**25**), and LiH···H_2O (**26**). The optimized geometries of these model complexes reflect the general trend observed in the larger series, viz., the

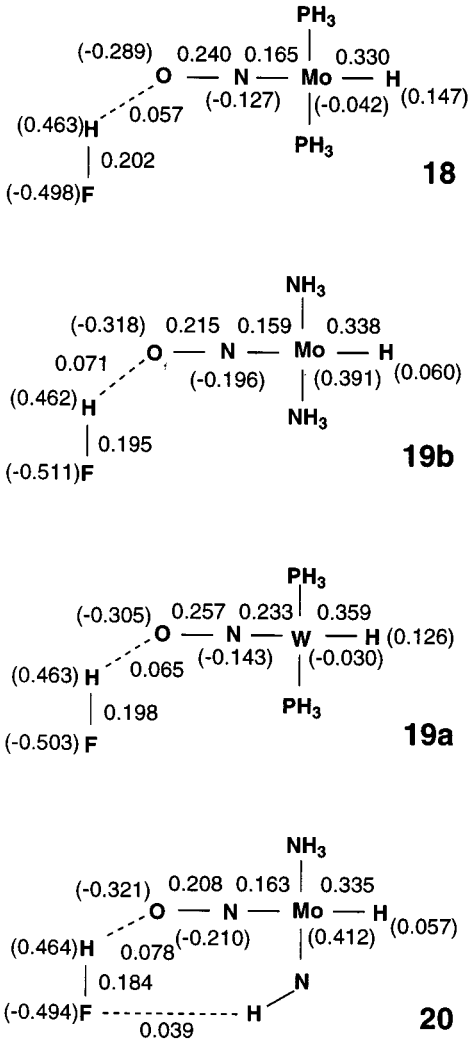

Figure 10. B3PW91 Mulliken overlap populations and charges (values in parentheses) of interacting fragments of **18**−**20**.

considerable lengthening of the H−R bond upon formation of the H···H complex. Calculations were carried out at the 6-31G* level[36] using the GAMESS package.[37] According to the ED analysis in Table 4, the conventional O···H bond can be classified as "ES > CT" since the electrostatic attraction is largest in magnitude, followed by charge transfer; polarization is considerably smaller. In contrast, the H···H bond in complexes **24** and **26** contains a much larger PL component and so might be termed "ES > CT ≈ PL". This term, the effect of distortion of the electron distributions, reflects the changes undergone by the M−H and H−R bonds when the H···H bond forms. Note also that the ES term is quite a bit larger in **24** and **26**.

A second issue is connected with the stereochemistry of the FH···O and FH···H complexes. The structure of the FH···O complex (C_s symmetry and θ(HON) = 103°) is guided by the direction of the lone pair on oxygen. Spherical symmetry of the interacting s atomic orbitals of the H···H bond does not impose any restrictions on the M−H···H angle α. Of course, both angles would increase in the case of proton donors more bulky than HF. To examine the latter question, the sensitivity of the energy of complexes **8** and **18** to the NOH and MoHH angles was calculated using B3PW91. The results reported in Figure 12 indicate only minor differences between the two complexes. An increase in the pertinent angle from its optimized value to 180° yields a destabilization of some 2.6 kcal/mol in either case. The two curves are nearly parallel to one another.

It is interesting that the H···O and H···H bond lengths change in different ways with increase of the corresponding angles. The H···O distance is enlarged smoothly with the increase of θ-(HON). In contrast, the H···H bond is shortened in the interval of 120°−140° but is elongated in the next interval of 140°−180°. This result may be explained by the scheme of equilibrium of M···HF and H···H interactions that was described above. In the first interval the increase of total energy of 0.9 kcal/mol is determined for the most part by the decrease of the M···HF interaction: the M···HF distance is elongated and the H···H bond is shortened.

Summary and Conclusions

Formation of the H···H interaction exhibits some of the characteristics of a conventional H-bond. The interaction energy between HF and $Mo(CO)_2(NO)(PH_3)_2H$ is fairly large, probably greater than 5 kcal/mol and maybe larger than 10. Upon formation of the complex, the HF bond of the proton donor is stretched, and a concomitant increase is also noted in the M−H bond of the hydride. Red shifts are also noted in the stretching frequencies associated with these bonds, and the overlap populations of both are diminished. Strengthening the σ-donor from PH_3 to NH_3 enhances the strength of the H···H interaction by several kcal/mol, as might be expected based on simple reasoning about a more nucleophilic hydride. In contrast, replacement of the Mo metal center by W has very little effect upon the complexation. The nature of the ligand trans to the hydride plays an important role. Replacement of NO by H not only increases the nucleophilic character of the transition metal but also leads from 18e to 16e structure and changes the basic geometry of the complex. In this case, the HF molecule adds to the complex in such a way that the H and F atoms are nearly equidistant from the Mo. In addition to any H···H interaction which is present, one also sees evidence of an agostic bond between the HF and a π-AO of Mo. It is notable that in a comparable sort of complex, in which the metal atom is replaced by B,[38] one also sees a "bending".

One can also obtain useful information by allowing a system like $Mo(CO)_2(NO)(PH_3)_2H$ to interact with a cationic subunit, e.g., H_3O^+. When this occurs, one of the protons of the latter moiety is essentially transferred to the metal complex and attaches itself to the hydride. The system may then be described as containing a neutral water bound to a complex in which H_2 acts as one of the ligands. With regard to steric factors, replacement of the axial NO by the bulkier Cl induces a displacement of the equatorial ligands PH_3, upward and toward

TABLE 4: HF/6-31G* Energy Components in kcal/mol for Complexes HNO···HF, LiH···HF, HNO···HOH, and LiH···HOH

							decomposition CT		decomposition PL	
structure	E_{ES}	E_{EX}	E_{PL}	E_{CT}	E_{MIX}	ΔE	accept.	HR	accept.	HR
HNO···HF	−6.22	3.76	−0.77	−1.74	0.04	−4.94	−1.60	−0.14	−0.68	−0.06
LiH···HF	−13.24	7.95	−2.75	−3.17	0.69	−10.52	−3.05	−0.12	−2.65	−0.38
HNO···HOH	−3.06	1.69	−0.26	−1.02	−0.02	−2.66	−0.96	−0.06	−0.19	−0.02
LiH···HOH	−10.97	7.88	−1.13	−2.42	0.36	−6.27	−1.48	−0.93	−0.68	−0.36

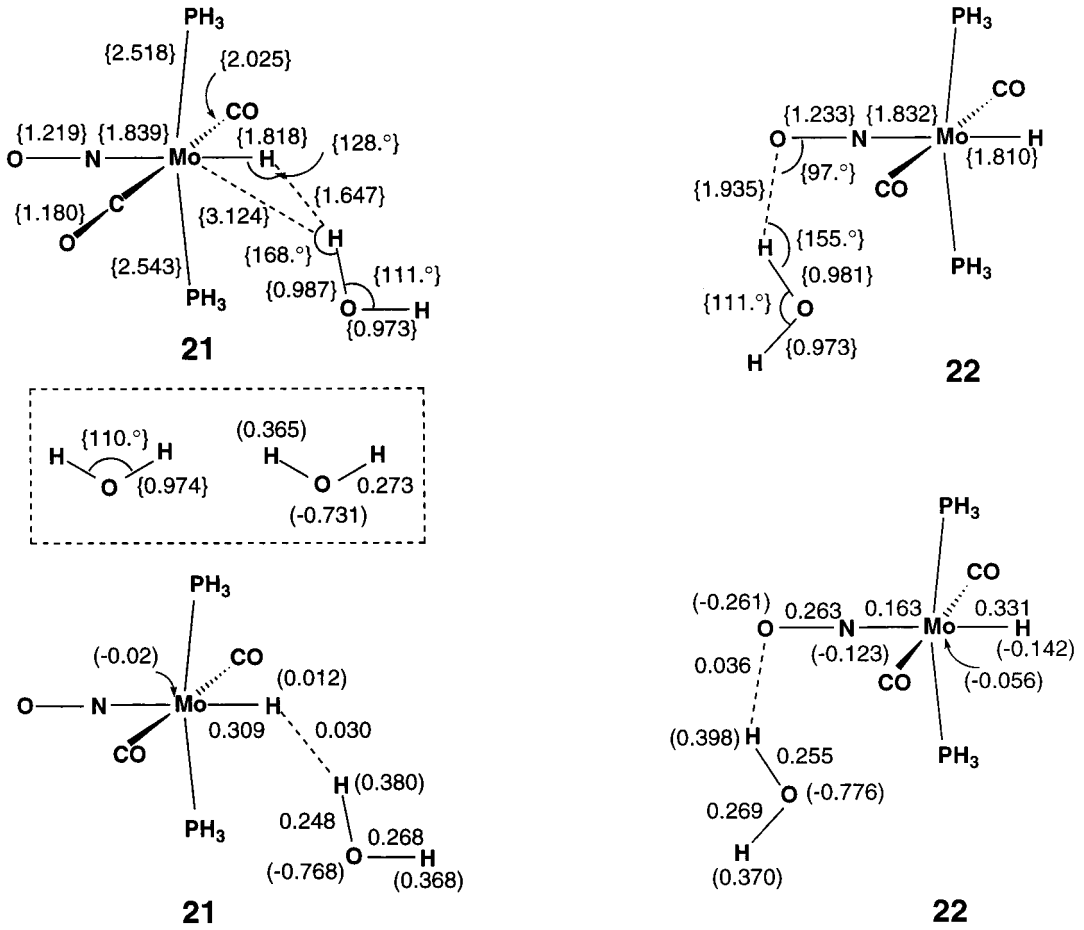

Figure 11. B3PW91 geometries (in Å and deg), Mulliken charges (values in parentheses), and overlap populations in **21**, **22**, and water molecule.

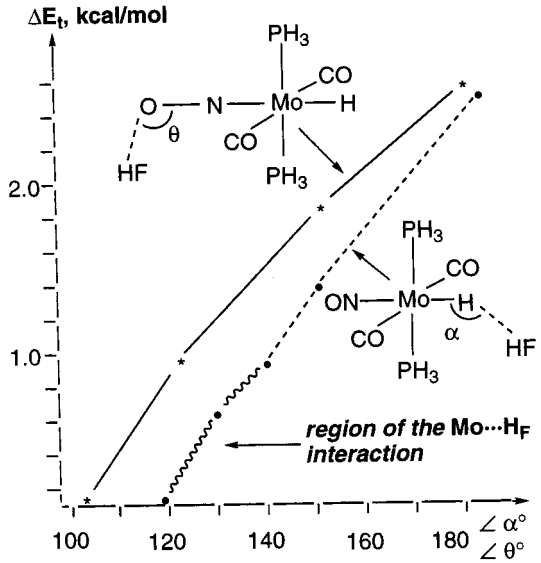

Figure 12. Variation of total energy with θ(NOH) and α(MoHH) angles relative to the energy of equilibrium structures for **18** and **8**.

the hydride. As a result of this steric crowding, the HF molecule cannot interact optimally with the hydride, weakening the H···H interaction.

As a point of comparison of the latter interaction with a conventional H-bond, the HF can also donate a proton to the oxygen end of a NO ligand. The H···H interaction is apparently preferred energetically, although the extent of this preference awaits more extensive calculations. A more basic ligand enhances either sort of interaction, probably due to greater nucleophilicity of the proton acceptor. Both sorts of interaction trigger a stretch of the HF bond. The conventional H-bond shows an increased negative charge on O and positive charge on the bridging hydrogen as the H-bond forms. In contrast, the positive charge on the bridging hydrogen becomes smaller in the H···H case.

Energy decomposition of smaller model complexes such as HNO···HF and LiH···HF reveals a fundamental distinction between H···H and H···O bonding. Whereas the latter conventional H-bonding attraction is composed primarily of electrostatic force, with a supplement from charge transfer, the H···H attraction has a more sizable contribution from polarization energy.

The H···H bonding energy increases with greater nucleophilicity of the hydride. The bond distance is shortened when the nucleophilic ability of the hydride hydrogen rises and is elongated when the nucleophilicity of the metal center is strengthened. From this point of view, the H···H complex can be considered in some sense as intermediate between a sort of η^2-H_2 and a dihydride structure, as illustrated in Figure 13. This correlation scheme eliminates the apparent contradiction that arose in connection with the H···H structure in complexes **1** and **3**, mentioned in the Introduction section. Indeed, complex **3**, which has strong π-acceptor and σ-donor ligands, appears to be a "pure" H···H-bonding complex. Complex **1** belongs to the "dihydride" type as there are σ-ligands only, and Re is rather nucleophilic in this case, although the steric factor hinders the Re···HR interaction.

When comparing the results of B3LYP, BLYP, and B3PW91 calculations on the hydride transition-metal complexes with intermolecular H···H bond, qualitatively similar conclusions are

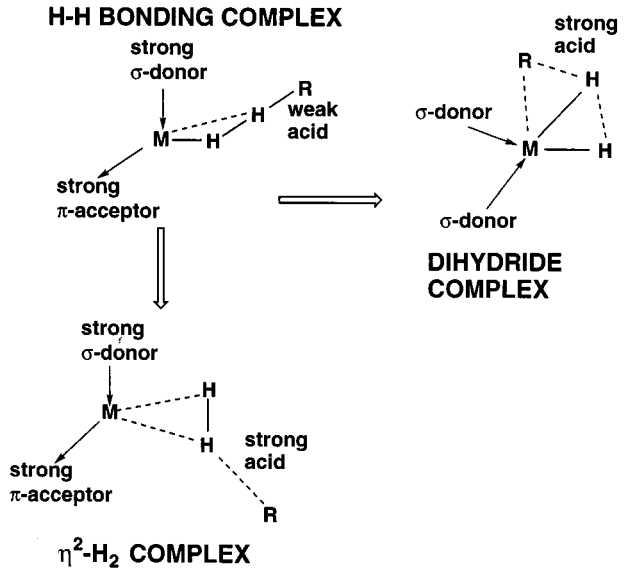

Figure 13. Correlation of the H···H, η^2-H_2, and dihydride structures.

reached by all three methods. However, the B3PW91 geometries and bond energies are in best agreement with experimental data; therefore, B3PW91 may be recommended for the calculations of H···H transition-metal complexes as a good compromise between accuracy and computational efficiency.

Acknowledgment. We are deeply grateful to members of the Epstein and Berke groups for extensive discussions and for sharing a preprint prior to publication. We thank the CAST program of NRC for support of this research.

References and Notes

(1) Liu, Q.; Hoffmann, R. *J. Am. Chem. Soc.* **1995,** *117*, 10108.

(2) Wessel, J.; Lee, J. C.; Peris, E.; Yap, G. P. A.; Fortin, J. B.; Ricci, J. S.; Sini, G.; Albinati, A.; Koetzle, T. F.; Eisenstein, O.; Rheingold, A. L.; Crabtree, R. H. *Angew. Chem., Int. Ed. Engl.* **1995,** *34*, 2507.

(3) Shubina, E. S.; Belkova, N. V.; Krylov, A. N.; Vorontsov, E. V.; Epstein, L. M.; Gusev, D. G.; Niedermann, M.; Berke, H. *J. Am. Chem. Soc.* **1996,** *118*, 1105.

(4) Belkova, N. V.; Shubina, E. S.; Ionidis, A. V.; Epstein, L. M.; Jacobsen, H.; Messmer, A.; Berke, H. *Inorg. Chem.* **1997,** *36*, 1522.

(5) Richmond, T. G.; Basolo, F.; Shriver, D. *Organometallics* **1982,** *1*, 1624.

(6) Chong, D. P.; Langhoff, S. R. *J. Chem. Phys.* **1986,** *84*, 5606. Raghavachari, K.; Truks, G. V.; Pople, J. I.; Head-Gordon, M. *Chem. Phys. Lett.* **1989,** *157*, 479.

(7) Parr, R. G.; Yang, W. *Density-Functional Theory of Atoms and Molecules*; Oxford University: New York, 1989. *Density Functional Methods in Chemistry*; Labanowski, J. K., Andzelm, J., Eds.; Springer-Verlag: New York, 1991.

(8) Jonas V.; Thiel, W. *J. Chem. Phys.* **1996,** *105*, 3636.; **1995,** *102*, 8474.

(9) Bytheway, I.; Bacskay, G. B.; Hush, N. S. *J. Phys. Chem.* **1996,** *100*, 6023.

(10) Bytheway, I.; Bacskay, G. B.; Hush, N. S. *J. Phys. Chem.* **1996,** *100*, 14899.

(11) Frisch, M. J.; Trucks, G. W.; Schlegel, H. B.; Gill, P. M. W.; Johnson, B. G.; Robb, M. A.; Cheeseman, J. R.; Keith, T.; Petersson, G. A.; Montgomery, J. A.; Raghavachari, K.; Al-Laham, M. A.; Zakrzewski, V. G.; Ortiz, J. V.; Foresman, J. B.; Peng, C. Y.; Ayala, P. Y.; Chen, W.; Wong, M. W.; Andres, J. L.; Replogle, E. S.; Gomperts, R.; Martin, R. L.; Fox, D. J.; Binkley, J. S.; Defrees, D. J.; Baker, J.; Stewart, J. P.; Head-Gordon, M.; Gonzalez, C.; Pople, J. A Gaussian, Inc., Pittsburgh, PA, 1995.

(12) Becke, A. D. *Phys. Rev.* A **1988**, *38,* 3098

(13) Becke, A. D. *J. Chem. Phys.* **1993,** *98*, 5648.

(14) Lee, C.; Yang, W.; Parr, R. G. *Phys. Rev. B* **1988**, *37*, 785. Miechlish, B.; Savin, A.; Stoll, H.; Preuss, H. *Chem. Phys. Lett.* **1989,** *157*, 200.

(15) Perdew, J. P.; Wang, Y. *Phys. Rev. B* **1992,** *45*, 13244.

(16) Perdew, J. P. *Phys. Rev.* A **1988,** *38,* 3098.

(17) Ziegler, T.; Fan, L. *J. Chem. Phys.* **1991,** *95*, 7401.

(18) Delly, B.; Wrinn, M.; Lüthi, H. P. *J. Chem. Phys.* **1994,** *100*, 5785.

(19) Fan, L.; Ziegler, T. *J. Chem. Phys.* **1991,** *95*, 7401.

(20) Hay, P. J.; Wadt, W. R. *J. Chem. Phys.* **1985,** *82*, 270; **1985,** 82, 299. Wadt, W. R.; Hay, P. J. *J. Chem. Phys.* **1985,** *82*, 284; Dunning, T. H.; Hay, P. J. In *Modern Theoretical Chemistry*; Schaefer, III, H. F., Ed.; Plenum: New York, 1976; pp 1−28.

(21) Binkley, J. S.; Pople, J. A.; Hehre, W. J. *J. Am. Chem. Soc.* **1980,** *102*, 939. Dobbs, K. D.; Hehre, W. J. *J. Comput. Chem.* **1987,** *8*, 861.

(22) Minyaev, R. M. *Int. J. Quantum Chem.* **1994,** *49*, 105.

(23) Due to the inordinate flatness of the DFT surface, it was impossible to unambiguously identify **8b** as a true minimum. Nonetheless, the energy was stable to within 10^{-6} hartree at the point that the optimization was interrupted.

(24) Hehre, W. J.; Radom, L.; Schleyer, P. v. R.; Pople, J. A. *Ab initio Molecular Orbital Theory*; Wiley: New York, 1986.

(25) Cioslowski, J.; Surjan, P. R. *THEOCHEM* **1992,** *255*, 9.

(26) Maseras, F.; Morokuma, K. *Chem. Phys. Lett.* **1992,** *195*, 500.

(27) McKee, M. L. *J. Am. Chem. Soc.* **1993,** *115*, 2818.

(28) Jost, A; Rees, B. *Acta Crystallogr.* **1975**, *B31*, 2649.

(29) Li, J.; Schreckenbach, G.; Ziegler, T. *J. Phys. Chem.* **1994,** *98*, 4838.

(30) Jean, Y.; Eisenstein, O.; Volarton, F.; Maouche, B.; Sefta, F. *J. Am. Chem. Soc.* **1986,** *108*, 6587.

(31) (a) The potential energy surface surrounding complex **13** is very flat; consequently, the search for minima is problematic. In this case, the geometry of **13** cannot be categorically defined as a minimum on the surface but would certainly be close to one. (b) Arndtsen, B. A.; Bergman, R. G.; Mobley, T. A.; Peterson, T. H. *Acc. Chem. Res.* **1995**, *28*, 154.

(32) Khalsa, G. R. K.; Kubas, G. J.; Unkefer, C. J.; Sluys, L. S. Van Der; Kubat-Martin, K. A. *J. Am. Chem. Soc.* **1990,** *112*, 3855.

(33) Scheiner, S. *Acc. Chem. Res.* **1994,** *27*, 402.

(34) Baerends, E. J.; Ellis, D. E.; Ros, P. E. *Chem. Phys.* **1973,** *2*, 41. teVelde, G.; Baerends, E. J. *J. Comput. Phys.* **1992,** *99*, 84.

(35) Kitaura, K.; Morokuma, K. *Int.J. Quantum Chem.* **1976,** *10*, 325.

(36) Hariharan, P. C.; Pople, J. A. *Chem. Phys. Lett.* **1972,** *66*, 217.

(37) Schmidt, M. W.; Baldridge, K. K.; Boatz, J. A.; Elbert, S. T.; Gordon, M. S.; Jensen, J. H.; Koseki, S.; Matsunaga, N.; Nguyen, K. A.; Su, S. J.; Windus, T. L.; Dupuis, M.; Montgomery, J. A. *J. Comput. Chem.* **1993,** *14*, 1347−1363.

(38) Richardson, T. B.; de Gala, S.; Crabtree, R. H.; Siegbahn, P. E. M. *J. Am. Chem. Soc.* **1995,** *117*, 12875−12876.